Available online at www.sciencedirect.com
SCIENCE DIRECT®
Journal of Power Sources 144 (2005) 461–466
JOURNAL OF POWER SOURCES
www.elsevier.com/locate/jpowsour

Hybrid modeling of lead–acid batteries in frequency and time domain

M. Thele[a,*], S. Buller[a], D.U. Sauer[a], R.W. De Doncker[a], E. Karden[b]

[a] *Electrochemical Energy Conversion and Storage Systems Group, Institute for Power Electronics and Electrical Drives (ISEA), RWTH Aachen University, Jaegerstrasse 17-19, D-52066 Aachen, Germany*
[b] *Ford Motor Company, Germany*

Available online 13 January 2005

Abstract

This paper presents an improved impedance-based non-linear simulation model for lead–acid batteries. The parameterization of impedance-based models is difficult for operation profiles with high Ah throughput in short times. Such conditions result in non-steady-state conditions and do not allow precise measurements of impedance parameters. Therefore, the model has been extended by an electrolyte transport model which describes the generation and the transport of sulfuric acid inside the porous electrodes. This expands the model validity as higher Ah throughputs can be simulated now. A description of the Matlab/Simulink implementation and its parameterization in the time domain is given. Furthermore, the advantages and the limits of the improved model are discussed. The model allows for precise modeling of automotive batteries, both in conventional applications and in vehicles with electrically assisted propulsion. It is therefore an important tool for the design of automotive power nets.

Keywords: Impedance spectroscopy; Impedance spectra; EISmeter; Frequency domain; Time domain; Modeling; Simulation; Diffusion; Electrolyte transport; State-of-charge; Lead–acid; VRLA

1. Introduction

Dynamical simulation models for electrochemical power sources are an important prerequisite for the simulation of systems like cars with electrically assisted propulsion or conventional automotive electrical systems. Fast computing and small parameterization effort are favorable. However, batteries show several characteristics that make a simple modeling with high precision nearly impossible. Batteries are not stationary, they are highly non-linear, and their dynamical behavior depends on different parameters like temperature, state-of-charge (SOC) or short term history [6,8].

Electrochemical impedance spectroscopy (EIS) is an adequate tool for the development and the parameterization of battery simulation models considering these aspects. Small-signal excitations and the evaluation of the system's response enables accurate investigations at nearly any working point. Reasonably good simulation models can be achieved without having proper information about the chemical compound as well as the inner geometrical design of the device. The computing time for the simulation is very short compared with physically or chemically based models.

The purely impedance-based battery model for lead–acid batteries [2] consists of elements that are related to physico-chemical processes. These processes are modeled in terms of inductances, capacitors and resistors with linear or non-linear dependency on temperature, SOC and/or battery current. The elements have to be parameterized by a systematic evaluation of impedance spectra recorded at various operating conditions. This approach shows very good agreement in particular for highly dynamical operation of the battery. However, for longer discharge events the model output may deviate significantly from the measured battery voltage. This limitation is inherent to the impedance method, because the measurement frequencies during model parameterization must be chosen to high enough to assume a quasi-stationary state of the battery during each measurement [2]. Consequently, dynamic processes that govern long-term discharge behavior of the

* Corresponding author. Tel.: +49 241 8096945.
E-mail address: te@isea.rwth-aachen.de (M. Thele).
URL: http://www.isea.rwth-aachen.de/ (M. Thele).

0378-7753/$ – see front matter © 2004 Elsevier B.V. All rights reserved.
doi:10.1016/j.jpowsour.2004.11.009

battery are not accessible for impedance methods. In particular, for lead–acid batteries acid concentration gradients as they develop during non-steady-state operation, are not covered by the purely impedance-based battery model.

This paper illustrates a hybrid modeling approach, which combines the impedance-based model and a basic electrolyte transport model. The former is developed and parameterized in the frequency domain, the latter in the time domain. The transport model describes the generation and the transport of sulfuric acid inside and between the porous electrodes. The hybrid model yields high precision in predicting the electrical battery performance even if strong variations of the acid concentration gradients occur. The parameterization and validation of the model has been carried out for a spiral-wound VRLA/AGM battery and typical operating conditions in a mild-hybrid vehicle. The same approach can be also employed for flooded lead–acid batteries.

2. The purely impedance-based simulation model

For a basic modeling approach, the Randles equivalent circuit can be employed ([8]; Fig. 1, left hand). The equivalent circuit is valid for both battery electrodes with differing parameters. It consists of an internal resistance R_i, an inductance L, a capacitance C and a non-linear resistance R. L is caused by the metallic connectors between the poles and the electrodes of the battery. The ohmic resistance R_i is due to the limited conductance of the contacts, the intercell connections, the grids, the active masses and the electrolyte. R_i depends on SOC, age and temperature of the battery. The parallel connection of the capacitance C and the non-linear resistance R represents the double layer capacity and the charge transfer resistance.

An equivalent circuit for a complete battery cell can be obtained by a series connection of two Randles circuits. A few modifications [2] have been carried out for the impedance-based lead–acid battery model, namely generalized capacitive elements (CPE: constant phase element [9]), a generalized dc-voltage source (considering the OCV potentials, $U_{0,\mathrm{cell}}$) and a parallel current path for gassing as the main side reaction.

For the parameter determination, several impedance spectra of the lead–acid battery have been measured at different working points considering not only the dependencies on the SOC and the battery temperature but also the current rate of the non-linear resistances. Therefore, different charge and discharge dc-currents have been superimposed during the impedance measurements. Fig. 2 shows several impedance spectra of a VRLA/AGM battery (measured at 70% SOC and room temperature) with varying bias dc-currents. The non-linearity of the battery, that is the non-linearity of the resistances R_1 and R_2 is obvious. More detailed information about the procedure of the impedance measurements, the evaluation of the impedance spectra and the modeling of the non-linearity can be found in [1,2].

For the model extension presented in this paper, the generalized dc-voltage source, which depends only on the SOC of the battery, has been replaced by a voltage source using the actual acid concentrations in both electrodes as the basis. The acid concentrations are calculated by means of an added electrolyte transport model.

3. Transport of sulfuric acid in VRLA batteries

An AGM/VRLA battery cell mainly consists of two porous electrodes with a highly porous separator in between. The electrolyte of the battery (sulfuric acid) is located inside the pores of these elements. The transport and the generation of the electrolyte can be characterized by means of the following differential equation [4]:

$$\varepsilon(t)\frac{\partial c(t)}{\partial t} = -c(t)\frac{\partial \varepsilon(t)}{\partial t} + \frac{\partial}{\partial x}\left(\varepsilon(t)^{\mathrm{ex}} D_{\mathrm{diff}}(c)\frac{\partial c(t)}{\partial x}\right) + G_{\mathrm{MR}} + G_{\mathrm{SR}} \quad (1)$$

where c corresponds to the acid concentration, ε to the porosity and D_{diff} is the diffusion coefficient of sulfuric acid [10]:

$$D_{\mathrm{diff}}(c)\,(\mathrm{cm}^2/\mathrm{s}) = (1.75 + 260c\,(\mathrm{mol/cm}^3)) \times 10^5 \times \exp\left(7.29 - \frac{2174\,\mathrm{K}}{T}\right) \quad (2)$$

G_{MR} and G_{SR} are sources of acid due to the main charge and discharge reaction and the side reaction (main reaction: "MR", side reaction: "SR"). c, ε, D_{diff}, G_{MR} and G_{SR} are functions of the spatial dimension x. The differential equation can be separated into three terms which influence the local acid concentration $c(t)$:

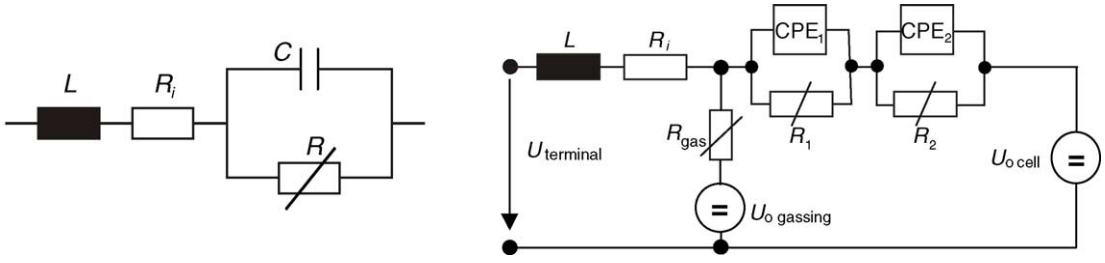

Fig. 1. Equivalent circuit of a battery half-cell (left hand); equivalent circuit for a complete lead–acid battery cell (right hand).

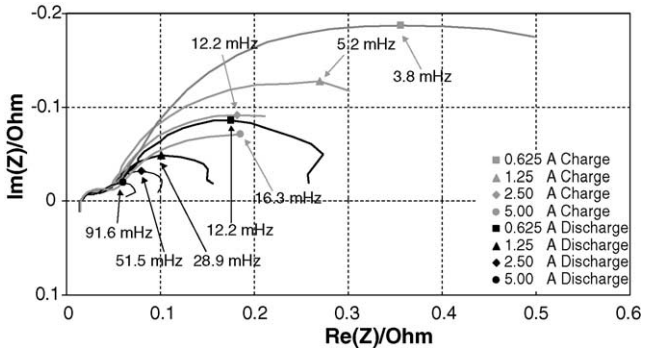

Fig. 2. Example of impedance spectra of a 36 V VRLA/AGM battery for different bias charge and discharge currents (SOC = 70%, 25 °C).

1. Diffusion:

$$\left[\frac{\partial}{\partial x}\left(\varepsilon(t)^{\mathrm{ex}} D_{\mathrm{diff}} \frac{\partial c(t)}{\partial x}\right)\right] \tag{3}$$

2. Changing of the porosity ε:

$$\left[-c(t)\frac{\partial \varepsilon(t)}{\partial t}\right] \tag{4}$$

3. Acid generation:

$$G_{\mathrm{MR}} + G_{\mathrm{SR}} \tag{5}$$

The two generation terms G_{MR} and G_{SR} are (with $t_+^0 = 0.72$, transference number):

$$\text{Positive electrode}: \quad G_{\mathrm{MR}} = \frac{3 - 2t_+^0}{2F} j_{\mathrm{MR}} \tag{6}$$

$$\text{Negative electrode}: \quad G_{\mathrm{MR}} = \frac{2t_+^0 - 1}{2F} j_{\mathrm{MR}} \tag{7}$$

$$\text{Positive and negative electrode}: \quad G_{\mathrm{SR}} = \frac{1 - t_+^0}{F} j_{\mathrm{SR}} \tag{8}$$

The porosity $\varepsilon_{\mathrm{pos/neg}}$ of the electrodes depends on the locally transferred amount of charge and, thus, the local state-of-charge. Assuming that the pores are completely filled with sulfuric acid, the change of the electrolyte volume inside the electrodes can be calculated using Eq. (9). The volume difference per mole of the charged or discharged active material ΔV_{m} amounts to 23.73 cm^3/mol at the positive electrode and to 30.64 cm^3/mol at the negative electrode. F corresponds to the Faradaic constant, j_{MR} to the current density (MR: main reaction) and n is according to the valence of the main reaction ($n = 2$). The maximum porosity of the electrodes is reached when the battery is fully charged:

$$\frac{\partial \varepsilon_{\mathrm{pos/neg}}(t)}{\partial t} = \frac{\Delta V_{\mathrm{m}}}{nF} j_{\mathrm{MR}} \tag{9}$$

In contrast to the electrodes porosity $\varepsilon_{\mathrm{pos/neg}}$, the porosity of the separator $\varepsilon_{\mathrm{sep}}$ is constant and no chemical or electrochemical reactions take place. Therefore Eq. (1) reduces as shown in Eq. (10). The separator provides electronic isolation but ionic conductivity:

$$\varepsilon(t)\frac{\partial c(t)}{\partial t} = \varepsilon(t)^{\mathrm{ex}} \frac{\partial}{\partial x}\left(D_{\mathrm{diff}}(c)\frac{\partial c(t)}{\partial x}\right) \tag{10}$$

4. The basic electrolyte transport model

Using the differential equation (1) for modeling, a fine spatial discretization of the battery cell would be necessary. However, for the sake of computing speed, a simplified spatial resolution with only three elements (positive/negative electrode, separator) has been chosen. The employed modeling approach of the battery cell is given Fig. 3 (right hand). It is of relevance to consider the electrodes half width due to the symmetry of the plate stack. The design of the battery under investigation is schematically illustrated on the left hand (Optima battery VRLA/AGM).

An adaptation of Eq. (1) is necessary due to the rough discretization. Therefore, the porosity ε and the diffusion coefficient D_{diff} are assumed to be only marginally dependent on x. Using the product rule, Eq. (1) simplifies to:

$$\frac{\partial(c(t)\varepsilon(t))}{\partial t} = \varepsilon(t)^{\mathrm{ex}} D_{\mathrm{diff}}(c)\frac{\partial^2 c(t)}{\partial x^2} + G_{\mathrm{MR}} + G_{\mathrm{SR}} \tag{11}$$

An approach to solve this equation can be found in [7]. The change of the acid concentration inside the electrodes is assumed to be linearly dependent on the difference of the acid concentrations between the positive electrode and the separator or the negative electrode and the separator, respectively. The acid concentration inside the separator is calculated by a material balance. The calculated concentrations are mean values for the total elements. The following equations can be found where d_{pos}, d_{neg} and d_{sep} correspond to the thickness of the electrodes and the separator:

$$c_{\mathrm{pos/neg}}(t) = \frac{\int \left(\varepsilon_{\mathrm{pos/neg}}(t)^{\mathrm{ex}} D_{\mathrm{diff}}(c_{\mathrm{pos/neg}}) \frac{\Delta c(t)}{\Delta x^2} + G_{\mathrm{MR(pos/neg)}} + G_{\mathrm{SR(pos/neg)}}\right) \mathrm{d}t}{\varepsilon_{\mathrm{pos/neg}}(t)} \tag{12}$$

$$c_{\mathrm{sep}} = -\left(\int \varepsilon_{\mathrm{pos}}(t)^{\mathrm{ex}} D_{\mathrm{diff}}(c_{\mathrm{pos}}) \frac{\Delta c(t)}{\Delta x^2} \mathrm{d}t\right) \frac{\varepsilon(t)_{\mathrm{pos}}}{\varepsilon_{\mathrm{sep}}} \frac{d_{\mathrm{pos}}}{d_{\mathrm{sep}}} - \left(\int \varepsilon_{\mathrm{neg}}(t)^{\mathrm{ex}} D_{\mathrm{diff}}(c_{\mathrm{neg}}) \frac{\Delta c(t)}{\Delta x^2} \mathrm{d}t\right) \frac{\varepsilon(t)_{\mathrm{neg}}}{\varepsilon_{\mathrm{sep}}} \frac{d_{\mathrm{neg}}}{d_{\mathrm{sep}}} \tag{13}$$

This approach allows high computing speed and can easily be implemented into the given impedance-based battery model. Only the old dc-voltage calculation ('$U_{0,\mathrm{cell}}$'; Fig. 1, right hand) has to be replaced. The new calculation of the dc-voltage corresponds to the difference of the negative and the positive potential (Eq. (14)) which can be calculated from the simulated acid concentrations inside the respective electrodes using Eqs. (15) and (16). For this calculation, the con-

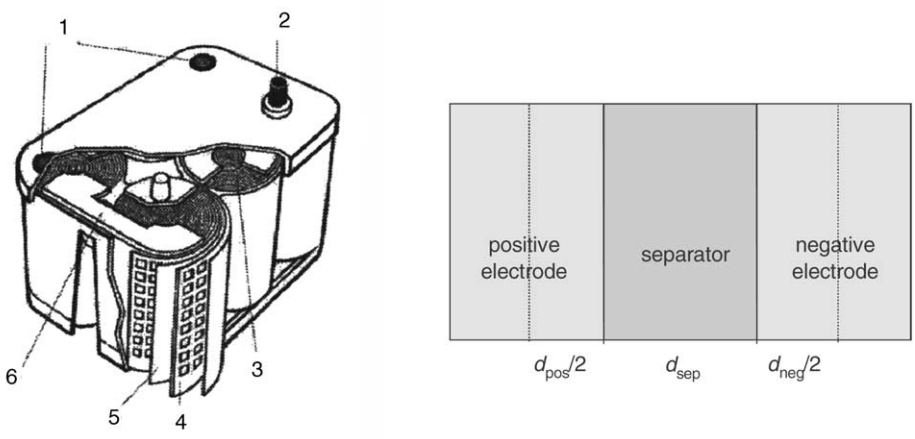

Fig. 3. Left hand figure—schematic of a VRLA/AGM battery of the spiral-wound type: (1) valves, (2) terminals, (3) spirally wound electrode pack, (4) punched lead grid, (5) AGM separator, (6) cast-on straps and intercell connectors [5]; right hand figure—simplified model of the battery cell used for the investigations on electrolyte transport.

centrations c (mol/cm^3) have to be converted into molalities m (mol/kg) (Eq. (17)) [10]:

$$U_{0,\text{cell}} = \phi_{0,\text{pos}} - \phi_{0,\text{neg}} \tag{14}$$

$$\phi_{0,\text{pos}}\,(\text{V}) = 1.628194 + 0.073924\log m + 0.033120\log^2 m + 0.043220\log^3 m + 0.021567\log^4 m \tag{15}$$

$$\phi_{0,\text{neg}}\,(\text{V}) = -0.2946 - 0.073595\log m - 0.030531\log^2 m - 0.030552\log^3 m - 0.012045\log^4 m \tag{16}$$

$$m = 1.00322\times10^3 c\,(\text{mol/cm}^3) + 3.55\times10^4 (c\,(\text{mol/cm}^3))^2 + 2.17\times10^6 (c\,(\text{mol/cm}^3))^3 + 2.06\times10^8 (c\,(\text{mol/cm}^3))^4 \tag{17}$$

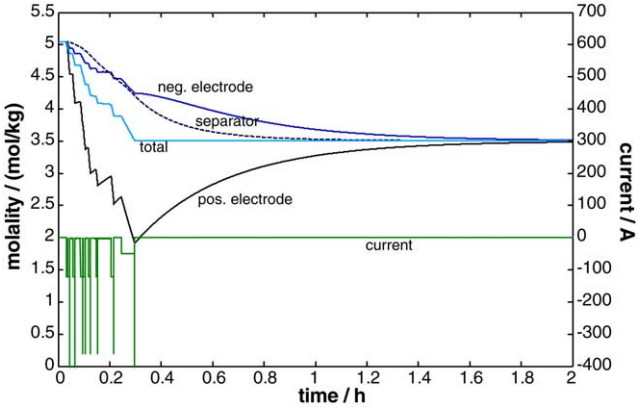

Fig. 4. Simulated acid molalities (inside the electrodes and the separator) for a stop/start load profile in a passenger car with high loads (calculated by the hybrid model); total molality (mean value, calculated by the purely impedance-based battery model) for comparison.

As an example, the simulated acid molalities (positive/negative electrode and separator) are illustrated in Fig. 4 for a load profile that represents a battery application in a stop/start (engine idle-off) passenger car with high loads. Significant gradients between the electrodes and the separator and the equalization process during rest periods become apparent. Moreover, the average molality (calculated by the purely impedance-based battery model, no spatial resolution) is given which corresponds to the SOC of the battery cell. A battery with 44 Ah nominal capacity and 70% initial SOC has been assumed.

5. Time-domain parameterization of the electrolyte transport model

To solve small deviations between simulated and measured battery voltage during long relaxation processes, an effective diffusion coefficient $D_{\text{diff,eff}}$ has been introduced. This coefficient replaces D_{diff} in Eqs. (12) and (13) and has been parameterized by a step-response method. Therefore, high-current discharge pulses (−100 A for 100 s) have been applied to the battery at different SOC (20, 40, 70 and 90%). Afterwards, simulations have been carried out by adapting the coefficient $D_{\text{diff,eff}}$ until a good agreement (simulation/measurement) could be observed during the relaxation periods. Fig. 5 documents this procedure at 90% SOC. The simulated voltage of the purely impedance-based battery model (without an electrolyte transport model) is given for comparison. The necessity to introduce $D_{\text{diff,eff}}$ is most probably due to the rough simplification of the transport model. However, the time-domain parameterization of the transport model is still simple and convincing results (achieved in short computing times) can be presented.

Some geometric parameters of the electrodes and the separator have to be known (thickness, porosity and the geometric surface (height × width)). Missing information can be at least

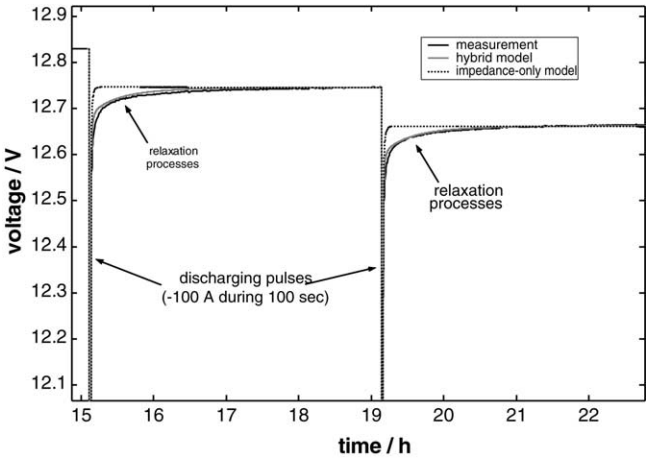

Fig. 5. High-current discharge pulses (100 A for 100 s, 90% SOC at the beginning); evaluation of the relaxation of the battery voltage for the determination of $D_{\text{diff,eff}}$.

partly extracted from the already illustrated high-current discharge pulses. The relaxed battery voltages (e.g. at 15, 19 and 22 h) correspond to the homogeneous acid concentration. According to the discharged Ah (2.77 Ah), the total electrolyte mass and consequently the electrolyte volume can be calculated. Moreover, the decrease of the battery voltage during the discharge pulses can be evaluated. Since diffusion is negligible during this short pulses, the electrolyte volume inside the electrodes can be also calculated.

6. Simulation results and verification with measurements

The model parameters including the parameters of the electrolyte model (see previous section) have been kept fixed for the following verification profiles. At first, some highly

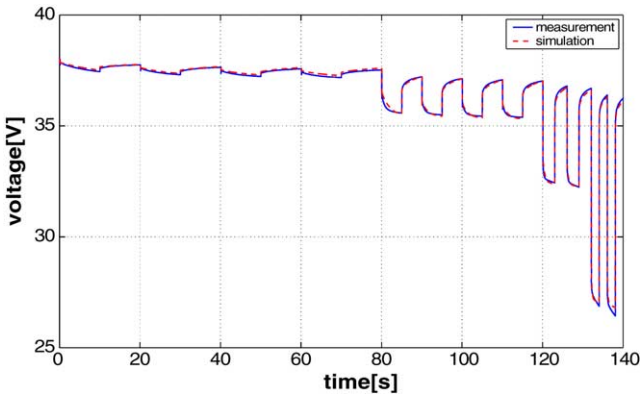

Fig. 6. High dynamical verification of the battery model (SOC = 70%, 25 °C).

dynamical verification measurements of the battery model are presented. Fig. 6 shows a measured and a simulated voltage profile which belong to repeated discharge pulses of −5, −50, −200 and −500 A with zero current periods in between. The battery under investigation was a 36 V VRLA/AGM battery. The discharged throughput amounted to 1.22 Ah which corresponds to less than 5% of the batter nominal capacity value (C_N = 27.5 Ah). The simulated voltage values show excellent agreement with the measured voltage profile for this highly dynamic profile.

Three different high-current discharge pulses with −66, −100 and −200 A are illustrated in Fig. 7. It becomes apparent that not only the relaxation periods after discharging can be simulated very accurately (relaxation processes are considered by the new hybrid model) but also the voltage drop during discharging.

Finally, Fig. 8 shows the measured and the simulated battery voltage for a load profile that represents a battery application in a stop/start (engine idle-off) passenger car with high loads. The battery was an automotive VRLA/AGM type

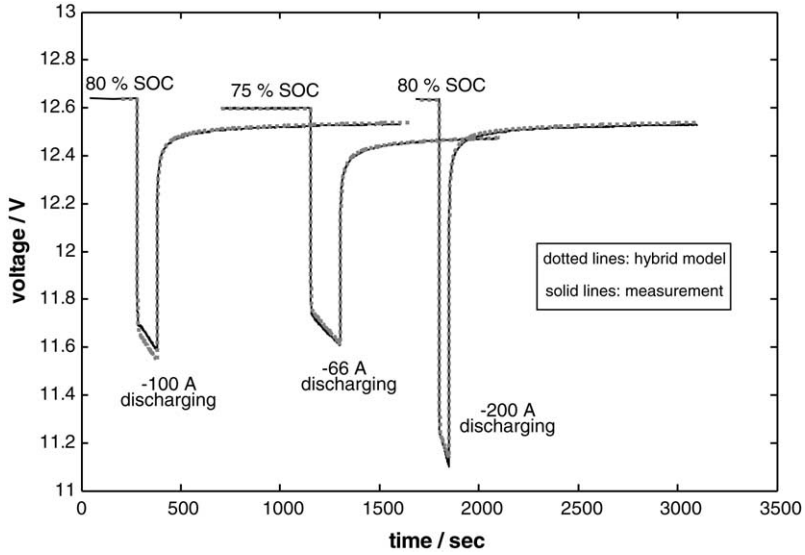

Fig. 7. Illustration of three different high-current discharging pulses (−66, −100 and −200 A) with a long relaxation period afterwards.

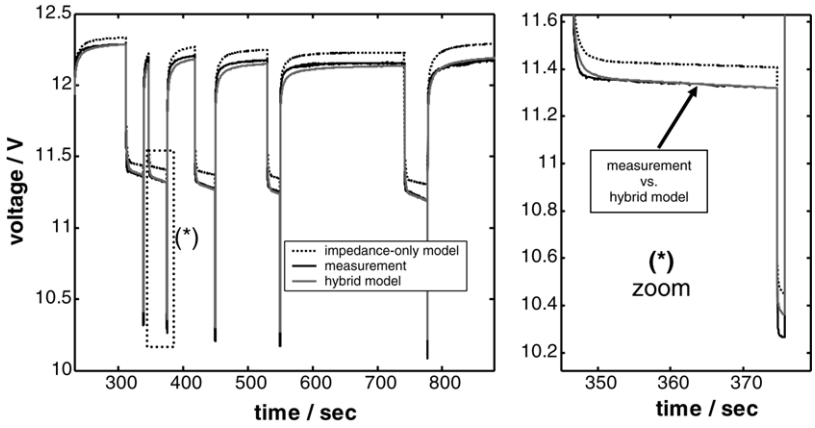

Fig. 8. Measured and simulated voltage responses.

(U_N = 12 V, C_N = 44 Ah). It can be expected that this profile will cause significant acid concentration gradients within each electrode pair. Therefore, the purely impedance-based model and the new hybrid model are compared additionally in this figure.

The dotted lines in the diagrams illustrate that the validity of the purely impedance-based simulation model is restricted to small SOC variations. The hybrid model, which includes the new transport model (solid gray line), fits the experimental battery voltage significantly better. Not only the voltage under load, but also the relaxation of the battery voltage during rest periods can be simulated more accurately.

7. Discussion

An improvement of an impedance-based non-linear simulation model for lead–acid batteries has been presented. The model has been extended by an electrolyte transport model, which describes the generation and the transport of sulfuric acid inside and between the porous electrodes. The implementation and its parameterization in the time domain have been described.

The comparison of the purely impedance-based battery model and the new hybrid model in Fig. 8 documents the remarkable improvement of the model's validity range. This advancement could be reached although the spatial resolution of the transport model – and thus, numerical efforts – was restricted to a minimum.

References

[1] S. Buller, M. Thele, E. Karden, R.W. De Doncker, Impedance-based non-linear dynamic battery modeling for automotive applications, J. Power Sources 113 (2003) 422–430.
[2] S. Buller, Impedance-based simulation models for energy storage devices in advanced automotive power systems, Dissertation Thesis, RWTH Aachen, 2002, ISBN 3-8322-1225-6.
[4] T.V. Nguyen, R.E. White, A mathematical model of a hermetically sealed lead-acid cell, Electrochim. Acta 38 (7) (1993) 935–945.
[5] D. Berndt, Valve-regulated lead-acid batteries, J. Power Sources 100 (2001) 29–46.
[6] D. Berndt, Bleiakkumulatoren, ISBN 3-18-400534-8.
[7] P. Ekdunge, A simplified model of the lead-acid battery, J. Power Sources 46 (1993) 251–262.
[8] J.O'M. Bockris, A.K.N. Reddy, M. Gamboa-Aldeco, Modern electrochemistry, in: Fundamentals of Electrodics, 2nd ed., vol. 2A, Kluwer Academic Publishers, 2000, p. 1425.
[9] J.R. Macdonald (Ed.), Impedance Spectroscopy, Emphasizing Solid Materials and Systems, Wiley, 1987, ISBN 0-471-83122-0.
[10] H. Bode, Lead-acid Batteries, Wiley, 1977, ISBN 0-471-08455-7.